A Novel Method for the Correlation of Histological Slides and MRI Imaging of the Prostate using 3D Vertex Models

Tom Bisson
University of Applied Sciences
Iris Piwonski
Charite Universitatsmedizin Berlin
Sebastian Lohmann
Hochschule fur Technik und Wirtschaft Berlin
Norman Zerbe
Charite Universitatsmedizin Berlin
Andreas Maxeiner
Charite Universitatsmedizin Berlin
David Horst
Charite Universitatsmedizin Berlin
Peter Hufnagl
Charite Universitatsmedizin Berlin
Tobias Penzkofer
Charite Universitatsmedizin Berlin
Sefer Elezkurtaj (sefer.elezkurtaj@charite.de)

Research

Keywords: Histology-MRI Correlation, Prostate Carcinoma, 3D Model

Posted Date: March 13th, 2020

DOI: https://doi.org/10.21203/rs.3.rs-17082/v1

RESEARCH

A Novel Method for the Correlation of Histological Slides and MRI Imaging of the Prostate using 3D Vertex Models

Tom Bisson[1,2*], Iris Piwonski[2], Sebastian Lohmann[1], Norman Zerbe[2], Andreas Maxeiner[3], David Horst[2], Peter Hufnagl[1,2], Tobias Penzkofer[4,5] and Sefer Elezkurtaj[2]

Abstract

Background: The evaluation and improvement of MRI-based grading schemes such as PI-RADS requires the correlation of histological findings with MRI images. Several approaches have been described to join the two modalities. However, these approaches have in common that they all require modification of the pathology workflow. Here, we describe a novel method to utilize vertex models for the correlation of histological findings with MRI images without affecting the histological sectioning protocol.

Methods: Three patients with prostate cancer who underwent radical prostatectomy as well as presurgical MRI were selected. Prostates are segmented on the MRI images to extract a 3D vertex model using 3D Slicer. Histological sectioning is then applied on the vertex model to yield reference planes for the tissue slides. Afterwards, slides and annotated tumor regions are aligned with the reference planes using the Coherent Point Drift algorithm. Carcinomas can then be visualized in 3D using the three different techniques of block representation, convex hull and Metaballs.

Results: 3D Slicer allows importing vertex models for segmentation purposes and thus the reconstructed tumors can be utilized as annotations in the original MRI images. Registration results are evaluated using the Jaccard index, which is computed by dividing the intersection area between tissue slide and reference plane by their union area. To evaluate the 3D reconstructions, the tumor-to-tissue ratio of the histological slides is computed. Block representation results in 76% of the original ratio while the convex hull causes a strong increase of 456%. The Metaball algorithm comprises a threshold parameter which affects the size of the 3D volume. Tumor-to-tissue ratios can be matched perfectly by selecting appropriate threshold values.

Conclusions: Our introduced method allows the correlation of histological findings with MRI images without the need to adapt the pathologists' workflow. In fact, the accuracy of 3D reconstruction techniques needs to be further optimized, but in return the method can be applied to the entire set of archive cases.

Keywords: Histology-MRI Correlation; Prostate Carcinoma; 3D Model

Background

Core needle biopsies are the gold standard for the diagnosis of prostate cancer (PCa). Biopsies are taken from a set of standard positions which can be extended to further biopsies related to lesions visible in MRI images. Several approaches exist to describe the visible lesions and estimate their malignancy. Using the multi-parametric prostate MRI (mpMRI), the Prostate Imaging and Reporting Data System (PI-RADS) can be utilized to classify morphological as well as functional features of the prostate in a non-invasive manner [1, 2]. In order to evaluate PI-RADS and alternative grading schemes, a method is required that allows for the transfer of histological findings to the corresponding regions in the MRI images. Since the histological slides cannot be well aligned with the MRI images, their correlation requires different preparation techniques [3]. Several approaches for the registration of histological slides to MRI images have been described, all of which entail special effort and changes in the processing routine. Furthermore, difficulties may arise when applying these techniques to archival cases which have been prepared according to the typical routine practice. Here, we describe a novel method for the correlation of histological slides with MRI images of the prostate using 3D vertex models.

Related Work

Several papers have been published about methods to correlate histological slides of the prostate with MRI data. Artificial reference points can be created by punctuating the prostate with thin needles which allows an inter-slide-registration to facilitate three-dimensional alignment [4]. Other approaches focus on performing the sectioning according to the recording angle of the MRI in order to directly register histological slides to the corresponding image [5, 6]. Most pathology institutes do not use whole mounts to avoid the various obstacles to histological processing and compatibility with archiving issues. For this reason, methods have been developed to register further subdivided tissue slices. This can be done by photographing the tissue slice before further subdivision. The image can then be used to reassemble the partial slices into a whole [7]. In order to register the joined tissue slices onto the corresponding MRI images, both can be converted into three-step grayscale images [8]. Finally, a device was introduced that allows the acquisition of MRI images of the ex vivo specimen with correspondingly sliced sections of the prostate, thus providing optimal data for correlation [9]. In addition to the methods for image registration, several publications describe patient-specific mounts derived from MRI data that allow high-precision sectioning of the prostate [10, 11, 12, 13].

Methods

Patients and image acquisition

Three different patients (age ranging from 59 to 75 years, Gleason 3 + 4 = 7 (ISUP 2), UICC stadium II and III (pT2c - pT3b), one patient with tumor in resection-boundaries (R1), all patients with perineural invasion (pN1) but without regional lymph node metastasis (pN0), lymphovascular or vascular invasion (L0V0)) who underwent radical prostatectomy have been chosen for the development of the method. All slides were digitalized using either the 3DHistech Pannoramic SCAN II (P150) or the Hamamatsu Nanozoomer and tumor regions were annotated using Cognition Master Professional Suite (v4.0) by VMscope. MRI was acquired using a Siemens Healthineers Skyra 3T MRI scanner and the prostate was

*Correspondence: tom.bisson@charite.de

[1]Center for Biomedical Image and Information Processing, University of Applied Sciences (HTW) Berlin, Wilhelminenhofstr. 75 A, 12459 Berlin, Germany

[2]Charité - Universitätsmedizin Berlin, corporate member of Freie Universität Berlin, Humboldt-Universität zu Berlin, and Berlin Institute of Health, Institute of Pathology, Charitéplatz 1, 10117 Berlin, Germany

Full list of author information is available at the end of the article

segmented with 3D Slicer v4.0 ([14]) and converted into a 3D vertex model.

Correlation of histological slides with MRI

Histological sectioning of the prostate is transferred to the MRI-derived 3D vertex model, followed by applying point set registration of the tissue slides to the approximated slices in the 3D model. To apply the sectioning to the 3D vertex model of the prostate, the open source 3D graphics suite Blender v2.79b is used. The supplied Boolean modifiers can be used to create sectional planes through 3D vertex models, allowing the sectioning of the ex vivo specimen to be fully transferred. Figure 1 illustrates this process by placing a section through a vertex model and then further dividing it into quarters.

In order to transfer the sectioning process to the 3D model with the necessary fidelity, the dissection protocol needs to be considered. Therefore, we created a JSON scheme that allows to digitally represent the individual sub-slices along with their position and slide ID. In addition, the fragmentation of the preparation according to the NeuroSAFE technique for intraoperative consultation ([15]) must be taken into account. To this end, we again used Blender's boolean modifier to remove the approximated NeuroSAFE segments from the specimen, as displayed in figure 2.

Applying the sectioning to the 3D models yields a set of approximated slices in 3D space, serving as a reference model for the registration of histological slides. Since the vertex model only consists of polygonal surfaces representing the prostate capsule, the reference slides are comprised solely of vertices and connecting edges. Therefore, the registration is limited to area and shape-based algorithms, such as coherent point drift (CPD) [16]. Since CPD requires pre-registration, all approximated sections are transferred to 2D space and then used for alignment and isotropic scaling of the histological sections. While translation and scaling are easy to compute, the determination of the best initial rotation is not trivial and therefore a series of incrementing rotation angles are used. The registration results are then compared using the Jaccard index ([17]) and best parameters are used for the final registration. Since we have found that an increasing number of polygon vertices leads to better registration results, we have implemented an algorithm to extrapolate polygons while maintaining their shape. Starting with the starting polygon, the longest edge is located and a new vertex is inserted at half the edges' length. This process is repeated until the target number of vertices has been reached for both the prostate slide outlines and the corresponding MRI reference polygons. Subsequently, all histological slides including tumor regions are registered on their reference polygons, as shown in Figure 3.

After registration, all tumor regions are retransferred to their associated positions in 3D space resulting in a set of polygons which represent the tumor outlines at the given locations. Based on these polygons the 3D tumor volume can be rendered from the annotations using different approaches. We implemented three rendering techniques and evaluated them by comparing the resulting tumor-to-tissue ratio with the ratio derived from the histological slides. In the first approach, all polygons are thickened according to the approximated tissue block size. Second, the convex hull of all polygons is computed. The third visualization aims at an interpolation of the tumor regions by utilizing Metaballs ([18]), which belong to the family of implicit surfaces. Only the latter approach can be parameterised in the form of a threshold value with which the merging behaviour of the Metaballs can be specified. A higher threshold penalizes the influence on other Metaballs and leads to smaller Metaballs in general.

Results

As deformations occur during the dissection and preparation of the prostate, the 3D models derived from the MRI differ from the ex vivo specimens and an additional change in shape is caused by the NeuroSAFE technique. To quantify the differences, we measured the ex vivo specimens of all three patients and compared them to the dimensions of the 3D models derived from MRI images. The results are given in table 1.

The alterations of size do not occur constantly along a particular axis or in a specific patient. This might be related to the NeuroSAFE technique, which involves removal of a posterolateral portion of the prostate following radical prostatectomy. However, the apicobasal axis is usually not affected by this technique and yet the deviation from the 3D model varies between 1.06% and 1.20%.

Polygon registration has been performed using CPD and the results were evaluated with the Jaccard index. All polygons have been extrapoliert to 500 points and 8 initial rotations each differing by an angle of 45° are used. The mean results of the three cases (Additional File 1: Registration Results) were 0.87, 0.86 and 0.91 with a standard deviation of 0.05, 0.07 and 0.04, respectively. Figure 4 shows representative images for the three volume rendering techniques.

All three techniques are evaluated by comparing the resulting tumor-tissue ratio with the one in the histological sections. The block representation results in a smaller ratio, making up only 76% of the reference values while the convex hull causes a strong increase of 456%. For the evaluation of the metaballs, the algorithm's threshold parameter must be considered. When each case is parametrized independently, the reference values can be matched explicitly by choosing individual thresholds of 1.824, 1.936 and 0.987. When the 3D reconstruction is complete, the vertex models can be reimported into 3D slicer to provide segmentation of the MRI images.

Discussion

To fit on standard size slides, tissue sections must be further subdivided, which can lead to additional tissue deformations and defects. Whole mount sectioning can be used to solve these problems ([19, 3]), which further complicates histological processing and archiving and is therefore only used by a small part of the urological pathologists [20]. Thus, we advocate a digital solution to realign the sub-slices prior to registration with the reference model.

Metaballs give the most realistic impression of the tumors when comparing the three visualization methods presented. The tumor-to-tissue ratio of the histological slides can be matched perfectly by adjusting the threshold parameter. However, an individually different value has to be determined for every case. Additionally, the detailed information about the tumor contours may be impaired. The convex hull is inappropriate for the visualization of PCa as it causes loss of information about the spatial distribution of multiple tumor foci. Using block representation, the tumor-to-tissue ratio is below the reference values. This might be related to both registration errors as well as the missing interpolation between the slices. While the visualization appears to be very schematic it is well-suited to describe the distribution and outline of the PCa. However, it does not provide a sound base for interpolation, since the underlying information does not allow a spatial assignment between the different tumor regions.

At the current stage, we did not consider different Gleason grades or growth patterns. All tumor lesions were treated equally, and no distinctions are made. This could be easily implemented in the block-wise visualization where every block is handled as an individual object and can be labelled independently. To

implement this with Metaballs, each group can be reconstructed separately, yielding groups of Metaballs for each occurring pattern or grade, respectively.

Conclusions

Radiological-pathological correlation is the cornerstone of any diagnostic paradigm, and highly valid datasets are essential for further refinement of diagnostic tools such as PI-RADS. Our introduced method can help to provide a large-scale database for the evaluation and improvement of PI-RADS by leveraging standard pathological diagnostic schemes without additional processing steps. For this purpose, the MRI-based tumor predictions can be imported into the 3D model and a comparison between the predictions and the histopathological findings can be made. The accuracy of our method requires further optimization, but in turn, it can be applied to the whole set our archival cases.

Abbreviations

MRI: Magnetic Resonance Imaging; mpMRI: multi-parametric MRI PI-RADS: Prostate Imaging-Reporting and Data System; PCa: Prostate Cancer; CPD: Coherent Point Drift.

Ethics approval and consent to participate

MRI data postprocessing was approved by Charité - Universitätsmedizin Berlin (EA1/271/16).

Consent for publication

Not applicable.

Availability of data and materials

All data is available from the corresponding author upon reasonable request.

Competing interests

The authors declare that they have no competing interests.

Funding

Not applicable.

Author's contributions

TB and SE developed methodology and performed experiments; TB, IP, SL, NZ, AM, DH, PH, TB and SE analyzed and interpreted data and wrote the manuscript; SE supervised the study. All authors read and approved the final manuscript.

Acknowledgements

We acknowledge support from the German Research Foundation (DFG) and the Open Access Publication Fund of Charité - Universitätsmedizin Berlin.

Author details

[1]Center for Biomedical Image and Information Processing, University of Applied Sciences (HTW) Berlin, Wilhelminenhofstr. 75 A, 12459 Berlin, Germany. [2]Charité - Universitätsmedizin Berlin, corporate member of Freie Universität Berlin, Humboldt-Universität zu Berlin, and Berlin Institute of Health, Institute of Pathology, Charitéplatz 1, 10117 Berlin, Germany. [3]Charité - Universitätsmedizin Berlin, corporate member of Freie Universität Berlin, Humboldt-Universität zu Berlin, and Berlin Institute of Health, Institute of Urology, Charitéplatz 1, 10117 Berlin, Germany. [4]Charité - Universitätsmedizin Berlin, corporate member of Freie Universität Berlin, Humboldt-Universität zu Berlin, and Berlin Institute of Health, Institute of Radiology, Augustenburger Platz 1, 13353 Berlin, Germany. [5]Berlin Institute of Health (BIH), Anna-Louisa-Karsch-Straße 2, 10178 Berlin, Germany.

References

1. Weinreb JC, Barentsz JO, Choyke PL, Cornud F, Haider MA, Macura KJ, et al. PI-RADS Prostate Imaging - Reporting and Data System: 2015, Version 2. Eur Urol. 2016 Jan;69(1):16–40.
2. Turkbey B, Rosenkrantz AB, Haider MA, Padhani AR, Villeirs G, Macura KJ, et al. Prostate Imaging Reporting and Data System Version 2.1: 2019 Update of Prostate Imaging Reporting and Data System Version 2. Eur Urol. 2019 Sep;76(3):340–351.
3. Fedorov A, Penzkofer T, Hirsch MS, Flood TA, Vangel MG, Masry P, et al. The role of pathology correlation approach in prostate cancer index lesion detection and quantitative analysis with multiparametric MRI. Acad Radiol. 2015 May;22(5):548–555.
4. Bart S, Mozer P, Hemar P, Lenaour G, Comperat E, Renard-Penna R, et al. MRI-histology registration in prostate cancer. In: Proceedings of Surgetica. Sauramps Medical Montpellier France; 2005. p. 361–367.
5. Chappelow J, Bloch BN, Rofsky N, Genega E, Lenkinski R, DeWolf W, et al. Elastic registration of multimodal prostate MRI and histology via multiattribute combined mutual information. Med Phys. 2011 Apr;38(4):2005–2018.
6. Xiao G, Bloch BN, Chappelow J, Genega EM, Rofsky NM, Lenkinski RE, et al. Determining histology-MRI slice correspondences for defining MRI-based disease signatures of prostate cancer. Comput Med Imaging Graph. 2011;35(7-8):568–578.
7. Orczyk C, Mikheev A, Rosenkrantz AB, Melamed J, Taneja SS, Rusinek H. Imaging of prostate cancer: a platform for 3D co-registration of in-vivo MRI ex-vivo MRI and pathology. Proc SPIE Int Soc Opt Eng. 2012 Feb;8316:83162M.
8. Kalavagunta C, Zhou X, Schmechel SC, Metzger GJ. Registration of in vivo prostate MRI and pseudo-whole mount histology using Local Affine Transformations guided by Internal Structures (LATIS). J Magn Reson Imaging. 2015 Apr;41(4):1104–1114.
9. Bourne RM, Bailey C, Johnston EW, Pye H, Heavey S, Whitaker H, et al. Apparatus for Histological Validation of In Vivo and Ex Vivo Magnetic Resonance Imaging of the Human Prostate. Front Oncol. 2017;7:47.
10. Shah V, Pohida T, Turkbey B, Mani H, Merino M, Pinto PA, et al. A method for correlating in vivo prostate magnetic resonance imaging

and histopathology using individualized magnetic resonance-based molds. Rev Sci Instrum. 2009 Oct;80(10):104301.

11. Turkbey B, Pinto PA, Mani H, Bernardo M, Pang Y, McKinney YL, et al. Prostate cancer: value of multiparametric MR imaging at 3 T for detection–histopathologic correlation. Radiology. 2010 Apr;255(1):89–99.
12. Trivedi H, Turkbey B, Rastinehad AR, Benjamin CJ, Bernardo M, Pohida T, et al. Use of patient-specific MRI-based prostate mold for validation of multiparametric MRI in localization of prostate cancer. Urology. 2012 Jan;79(1):233–239.
13. Priester A, Natarajan S, Le JD, Garritano J, Radosavcev B, Grundfest W, et al. A system for evaluating magnetic resonance imaging of prostate cancer using patient-specific 3D printed molds. Am J Clin Exp Urol. 2014;2(2):127–135.
14. Fedorov A, Beichel R, Kalpathy-Cramer J, Finet J, Fillion-Robin JC, Pujol S, et al. 3D Slicer as an image computing platform for the Quantitative Imaging Network. Magn Reson Imaging. 2012 Nov;30(9):1323–1341.
15. Schlomm T, Tennstedt P, Huxhold C, Steuber T, Salomon G, Michl U, et al. Neurovascular structure-adjacent frozen-section examination (NeuroSAFE) increases nerve-sparing frequency and reduces positive surgical margins in open and robot-assisted laparoscopic radical prostatectomy: experience after 11,069 consecutive patients. Eur Urol. 2012 Aug;62(2):333–340.
16. Myronenko A, Song X. Point set registration: coherent point drift. IEEE Trans Pattern Anal Mach Intell. 2010 Dec;32(12):2262–2275.
17. Jaccard P. Distribution de la flore alpine dans le bassin des Dranses et dans quelques régions voisines. Bull Soc Vaudoise Sci Nat. 1901;37:241–272.
18. Blinn JF. A generalization of algebraic surface drawing. ACM transactions on graphics (TOG). 1982;1(3):235–256.
19. Yamamoto H, Nir D, Vyas L, Chang RT, Popert R, Cahill D, et al. A Workflow to Improve the Alignment of Prostate Imaging with Whole-mount Histopathology. Acad Radiol. 2014 Aug;21(8):1009–1019.
20. Samaratunga H, Montironi R, True L, Epstein JI, Griffiths DF, Humphrey PA, et al. International Society of Urological Pathology (ISUP) Consensus Conference on Handling and Staging of Radical Prostatectomy Specimens. Working group 1: specimen handling. Mod Pathol. 2011 Jan;24(1):6–15.

Figures

Figure 1 Sectioning of 3D vertex models. Boolean Modifier in Blender for the intersection of a plane with the 3D vertex model of the prostate (a & b), followed by further subdivision into quarters (c).

Figure 2 NeuroSAFE technique on a vertex model. 3D vertex model of the prostate including NeuroSAFE sectional planes (a), and 3D vertex model after removal of the NeuroSAFE segments (b).

Figure 3 Slide registration. Registration of a histological slide (a) to its' 3D approximate with the coherent point drift algorithm. Annotated tumor regions are represented in blue and in the results (b) the slide outline is shown in yellow and the approximate in black.

Figure 4 Prostate tumor renderings. Three techniques for rendering tumor volumes in the prostate using (from left to right) block representation, convex hull and metaballs.

Table 1 Dimensions of the ex vivo specimens and the deviation in the MRI derived 3D models along the horizontal, antero-dorsal and apico-basal axis.

	Case 1		Case 2		Case 3	
Origin	Ex Vivo	MRI	Ex Vivo	MRI	Ex Vivo	MRI
Horizont.	50 mm	1.1%	50 mm	1.0%	53 mm	1.1%
Ant.-Dors.	41 mm	0.9%	42 mm	1.0%	46 mm	1.0%
Ap.-Basal	30 mm	1.2%	52 mm	1.1%	46 mm	1.2%

Tables

Additional Files

Additional file 1: Registration Results

The results of all registrations per case as .xlsx file (MS Excel).

Figures

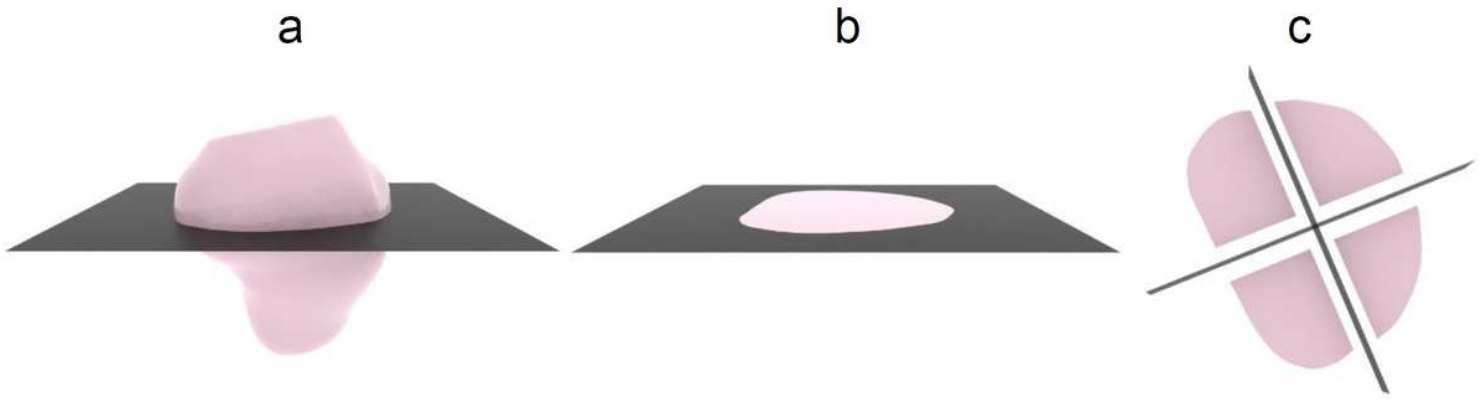

Figure 1

Sectioning of 3D vertex models. Boolean Modier in Blender for the intersection of a plane with the 3D vertex model of the prostate (a & b), followed by further subdivision into quarters (c).

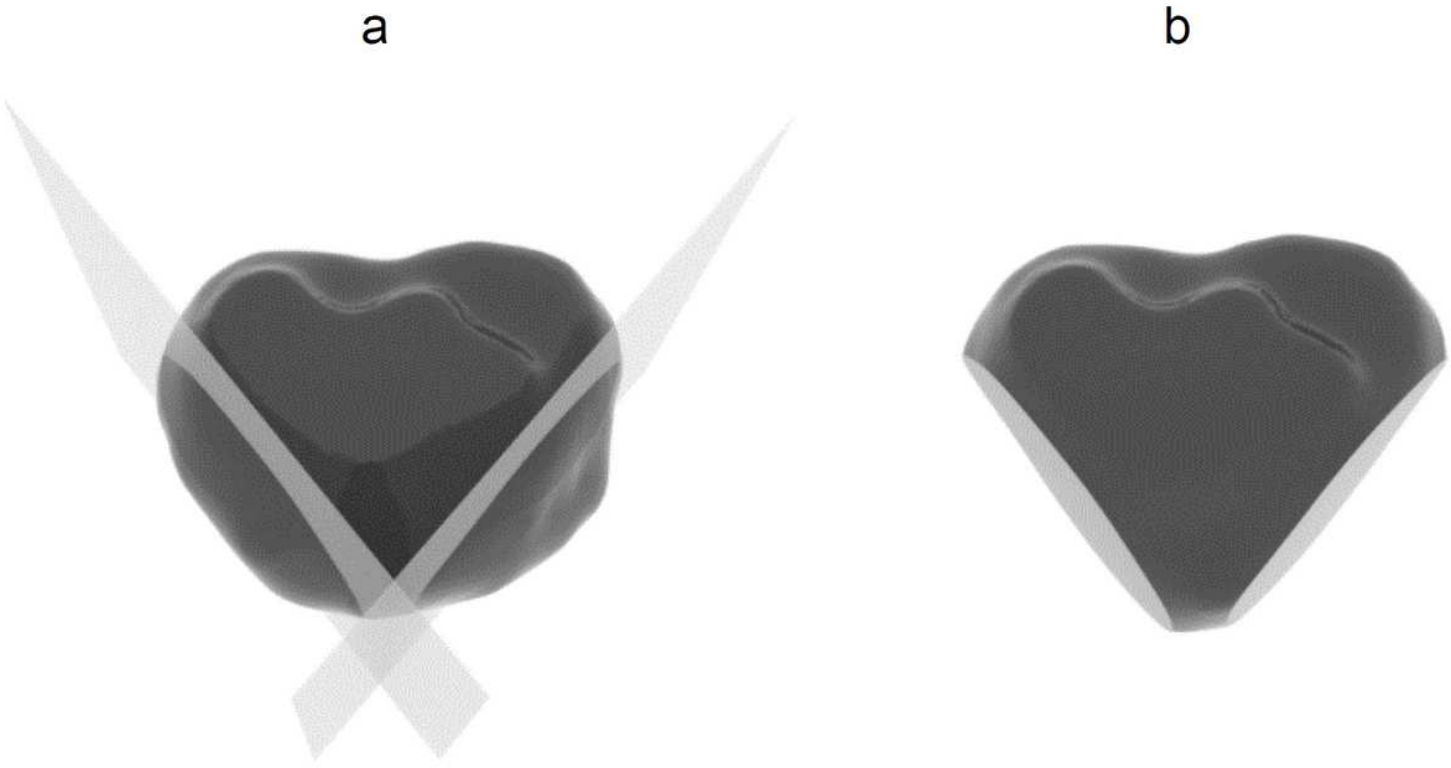

Figure 2

NeuroSAFE technique on a vertex model. 3D vertex model of the prostate including NeuroSAFE sectional planes (a), and 3D vertex model after removal of the NeuroSAFE segments (b).

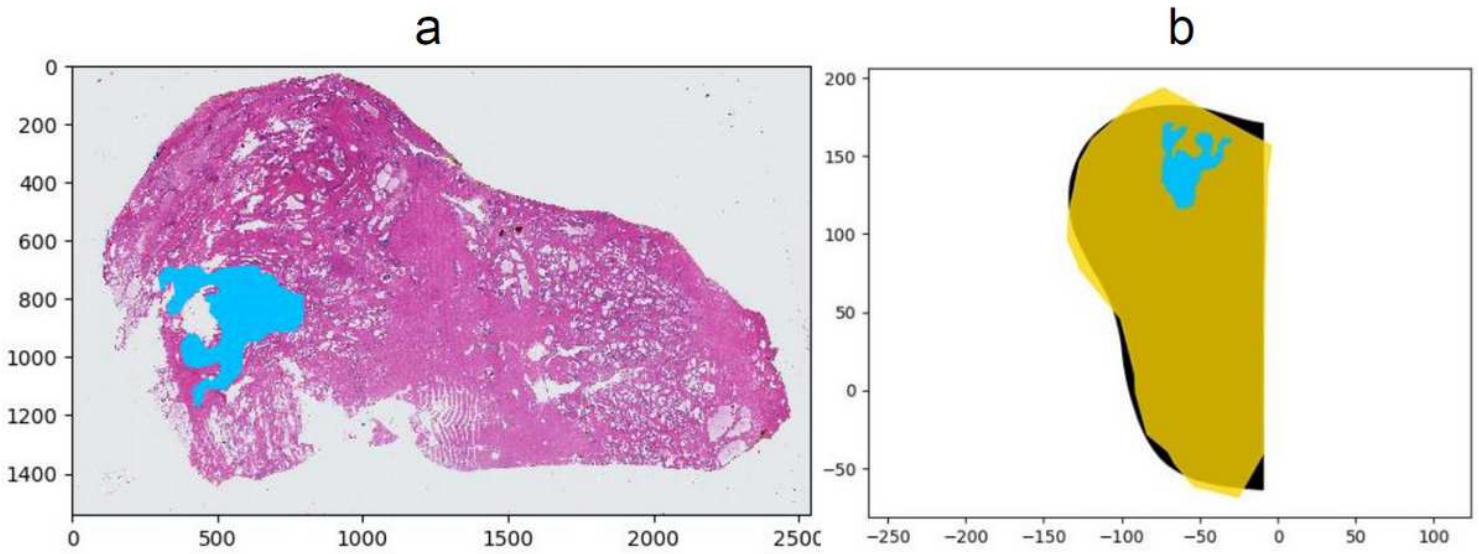

Figure 3

Slide registration. Registration of a histological slide (a) to its' 3D approximate with the coherent point drift algorithm. Annotated tumor regions are represented in blue and in the results (b) the slide outline is shown in yellow and the approximate in black.

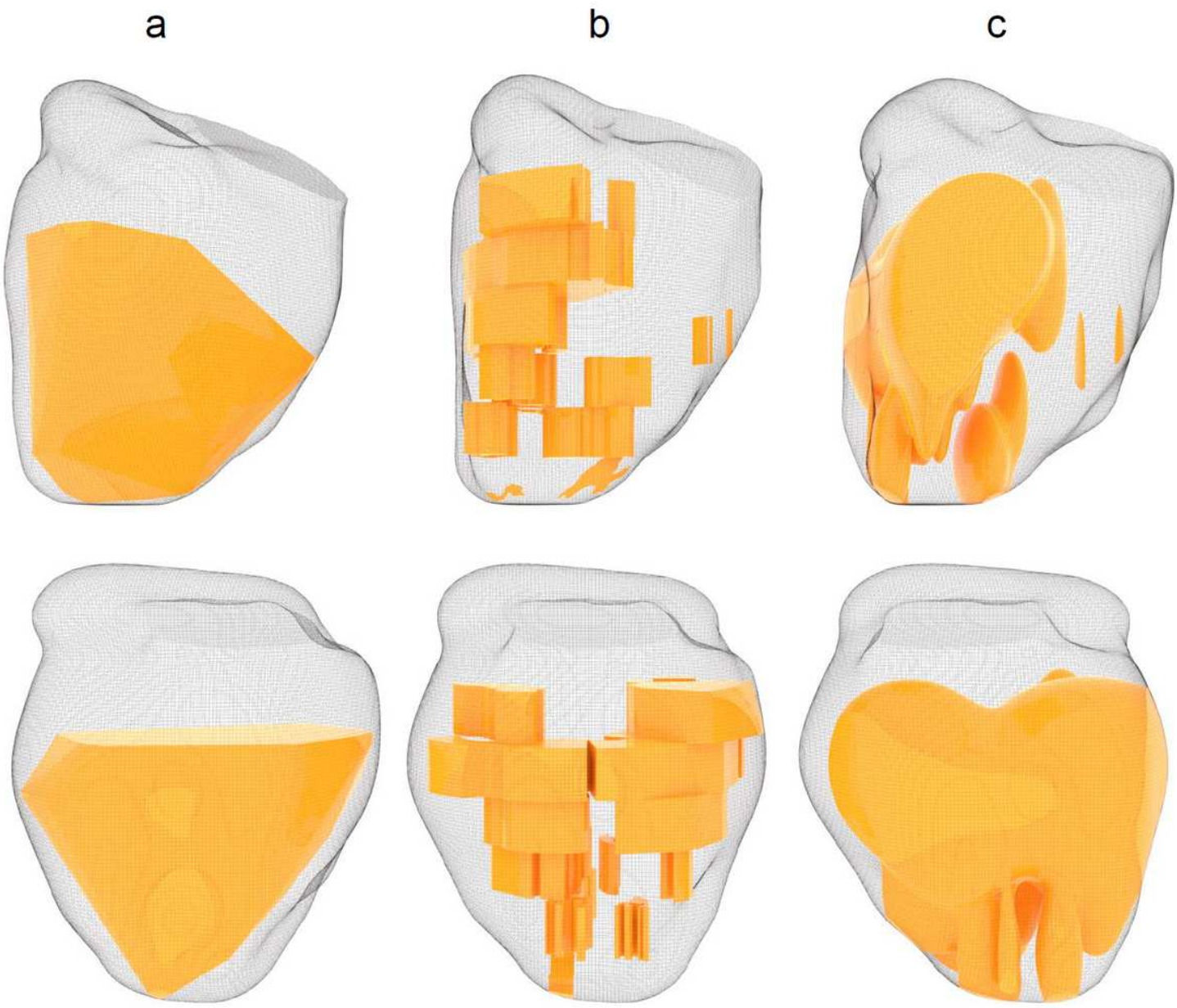

Figure 4

Prostate tumor renderings. Three techniques for rendering tumor volumes in the prostate using (from left to right) block representation, convex hull and metaballs.

Supplementary Files

This is a list of supplementary files associated with this preprint. Click to download.

- RegistrationResults.xlsx